LRP1 as a promising therapeutic target for gastrointestinal tumors: Inhibiting proliferation, invasion and migration of cancer cells

MENGYING ZHU[1*], HAO SHEN[2*], BILI WANG[2], YINGFEI HE[3], JIN CHEN[1], JUN REN[1], ZHEZHONG ZHANG[4] and XU JIAN[1]

[1]School of Medical Technology and Information Engineering, Zhejiang Chinese Medical University, Hangzhou, Zhejiang 310053; [2]Lab Center, The Children's Hospital Zhejiang University School of Medicine, Hangzhou, Zhejiang 310052; [3]Department of Pathology, The Second Affiliated Hospital of Zhejiang University School of Medicine, Hangzhou, Zhejiang 310009; [4]Department of Clinical Laboratory, The First Affiliated Hospital of Zhejiang Chinese Medical University, Hangzhou, Zhejiang 310006, P.R. China

Received May 21, 2023; Accepted August 1, 2023

DOI: 10.3892/ol.2023.14019

Abstract. Gastrointestinal (GI) cancers are the most common types of tumors worldwide. The lack of cancer biomarkers and targeted drug resistance are barriers to achieving effective cancer therapy. Low-density lipoprotein receptor-related protein 1 (LRP1) is a transmembrane protein that has multiple functions due to its ability to recognize different ligands; however, the role of LRP1 in GI cancer cells remains unclear. The present study aimed to investigate the role of LRP1 in GI tumors. The Cancer Genome Atlas database was used to analyze the potential correlation between expression of LRP1 and prognosis in patients with GI cancer. Bioinformatics analysis was utilized and the expression of LRP1 was simultaneously validated in GI cancer at the cellular level through western blot experiments. LRP1 was expressed at high levels in HGC-27, HepG2 and BxPC-3 cells. LRP1 expression in GI cancer cells was knocked down using lentivirus-mediated shRNA and the effects on biological functions were observed. LRP1 knockdown suppressed the proliferation, invasion and migration of GI cancer cells. LRP1 knockdown inhibited CD36 gene expression in HepG2 and BxPC-3 cells. LRP1 knockdown inhibited the proliferation, invasion and migration of GI cancer cells, suggesting that LRP1 may be a novel target for treatment of GI tumors.

Correspondence to: Professor Xu Jian, School of Medical Technology and Information Engineering, Zhejiang Chinese Medical University, 548 Binwen Road, Hangzhou, Zhejiang 310053, P.R. China
E-mail: 20061036@zcmu.edu.cn

Dr Zhezhong Zhang, Department of Clinical Laboratory, The First Affiliated Hospital of Zhejiang Chinese Medical University, 54 Post and Telegraph Road, Hangzhou, Zhejiang 310006, P.R. China
E-mail: zhangzhezhong2023@163.com

*Contributed equally

Abbreviations: GI, gastrointestinal; LRP1, low density lipoprotein receptor-related protein 1; TCGA, The Cancer Genome Atlas; CCK-8, Cell Counting Kit-8; CA19-9, carbohydrate antigen 19-9; LDLR, low-density lipoprotein receptor; KEGG, Kyoto Encyclopedia of Genes and Genomes; GO, Gene Ontology; COAD, colon adenocarcinoma; LIHC, liver hepatocellular carcinoma; PAAD, pancreatic adenocarcinoma; STAD, stomach adenocarcinoma; LV, lentiviral; shNC, short hairpin negative control; p, phosphorylated; EGFR, epidermal growth factor receptor; MMPs, matrix metalloproteinase

Key words: gastrointestinal cancer, low-density lipoprotein receptor-related protein 1, invasion, lipid absorption

Introduction

Low-density lipoprotein receptor-related protein-1 (LRP1) is a multifunctional endocytic receptor that participates in the metabolism of various extracellular ligands, such as platelet-derived growth factor and matrix metalloproteinase-9 (MMP-9), by regulating cell signaling pathways, such as the Wnt/β-catenin pathway, including enzymes involved in tumor invasion (1). Lipoprotein metabolic processes are activated in tumors and increased lipid uptake and storage in a variety of cancers contribute to rapid tumor growth (2).

Gastrointestinal (GI) cancer is among the most common malignancies worldwide and comprises esophageal, stomach, colorectum, liver and pancreatic cancer (3). A total of 4.9 million GI cancer cases and 3.5 million GI cancer-related deaths were estimated in 2020 (4). GI cancers account for 26% of global cancer incidence and 35% of all cancer-related deaths (4). Early stage treatment of GI cancer is mainly performed by surgical resection (5). Chemotherapy is the primary treatment for advanced GI cancers; however, the resistance of cancer cells to chemotherapy drugs leads to chemotherapy failure (6). Clinical diagnosis and treatment need novel biomarkers of GI cancer to allow for earlier detection. Feng *et al* (7) showed

that positive rates of α-fetoprotein and cancer antigen 19-9 (CA19-9) are relatively low in early-stage stomach cancer, while levels of carcinoembryonic antigen are an independent risk factor for poor prognosis of early-stage stomach cancer. Moreover, pancreatic cancer has a poor survival rate and the high mortality rate is attributed to the difficulty of making an early-stage diagnosis (8).

In a previous study, knocking down LRP1 in pancreatic cancer PANC-1 cells inhibited tumor cell proliferation (9). Gheysarzadeh *et al* (10) showed that upregulation of LRP1 is associated with poor prognosis and cell invasion in pancreatic cancer. In pancreatic cancer, lipoprotein metabolic process results in an increase in the levels of cholesterol and upregulation of low-density lipoprotein receptor (LDLR) in tumor cells (11). Pancreatic ductal adenocarcinoma has no obvious symptoms in the early stage of the disease, and diagnosis is difficult, which results in later-stage diagnosis of the disease and poor prognosis. Compared with low-grade astrocytoma, malignant glioma is characterized by notably higher levels of LRP1 mRNA and protein (12). Huang *et al* (13) showed that high expression of LRP1 is associated with low metastatic potential of hepatocellular carcinoma.

However, the specific role and molecular mechanism of LRP1 in GI tumor cells remains unclear. It is hypothesized that LRP1 is related to cholesterol uptake and the proliferation of tumor cells and the high expression of LRP1 may promote the proliferation of tumor cells. To verify this hypothesis, bioinformatics analysis was used to investigate the expression of LRP1 in GI tumors and its correlation with prognosis of patients with GI cancer. Subsequently, *in vitro* experiments were performed to evaluate the impact of LRP1 knockdown on GI cancer cell proliferation, migration and invasion.

Materials and methods

Bioinformatics analysis. RNA sequencing data for normal stomach, pancreas and liver from the Genotype-Tissue Expression database (gtexportal.org), and for stomach, pancreas and liver tumors from The Cancer Genome Atlas database (TCGA; portal.gdc.cancer.gov) were downloaded from the Xena portal (https://github.com/BD2KGenomics/toil) with data generated by the Toil pipeline management system (14). The enrichment data of Gene Ontology (GO; http://geneontology.org/) and Kyoto Encyclopedia of Genes and Genomes (KEGG) enrichment analysis pathway were derived from the KEGG website (www.kegg.jp). The analyses were performed using R (version 3.6.3; https://www.r-project.org/) with packages 'ggplot2' (version 3.3.3), 'survival' (version 3.2.10), 'survminer' (version 0.4.9), 'DESeq2' (version 3.3.3) and 'pROC' (version 1.17.0.1).

GSEA. Enrichment analysis was conducted using GSEA (version 4.2.2) software on data retrieved from the TCGA database (15,16). The analysis process involved the following steps: i) Calculating enrichment scores for each gene set; ii) sorting the gene sets based on the magnitude of their enrichment scores; iii) considering results as statistically significant if they met the criteria of $P<0.05$, false discovery rate (FDR) <25% and normalized enrichment score >1.0.

Cell lines and culture. HGC-27, HepG2 hepatoblastoma (cellosaurus.org/CVL_0027), BxPC-3 (authenticated through short tandem repeat analysis), PANC-1 and CaCo-2 cells, and HUVECs, were obtained from the Cell Bank of the Chinese Academy of Science (Shanghai, China). Cells were cultured in Dulbecco's Modified Eagle's medium or RPMI-1640 (both Gibco; Thermo Fisher Scientific, Inc.) supplemented with 10% fetal bovine serum (FBS; HyClone; Cytiva). All cell lines were cultured at 5% CO_2 and 37˚C.

Western blotting. The following primary antibodies were used for western blotting: LRP1 (cat. no. ab92544; 1:10,000; Abcam), ERK1/2 (cat. no. ab184699; 1:5,000, Abcam), phosphorylated ERK1/2 (p-ERK1/2; cat. no. ab201015; 1:5,000; Abcam), AKT (cat. no. ab38449; 1:10,000; Abcam), p-AKT (cat. no. ab81283; 1:10,000; Abcam), epidermal growth factor receptor (EGFR; cat. no. ab52849; 1:10,000; Abcam), MMP2 (cat. no. ab92536; 1:5,000; Abcam), MMP9 (cat. no. ab76003; 1:10,000; Abcam) and GAPDH (cat. no. ab8245; 1:5,000; Abcam). Horseradish peroxidase-conjugated anti-mouse (cat. no. GAM007; 1:5,000; Multi Sciences Biotech Co., Ltd.) or anti-rabbit IgG antibodies (cat. no. GAR007; 1:5,000; Multi Sciences Biotech Co., Ltd.) were used as secondary antibodies, and an enhanced chemiluminescent kit (Multi Sciences Biotech Co., Ltd.) was used for visualization. The total protein extraction buffer was prepared by mixing RIPA Lysis Buffer (cat. no. P0013B; Beyotime Institute of Biotechnology) with phenylmethanesulfonyl fluoride (cat. no. ST506; Beyotime Institute of Biotechnology) in a 1:1 ratio. The total protein was obtained all aforementioned cell lines. The protein concentration was determined after total protein extraction using the BCA Protein Assay Kit (cat. no. P0012; Beyotime Institute of Biotechnology). Each lane was loaded with 100 μg total protein and separated on a gels using SDS-PAGE (6% stacking gel, 10% separating gel). Transfer to a PVDF membrane (cat. no. ISEQ00010; MilliporeSigma) was performed at 200 mA constant current using the Biorad Powerpac Basic 164-5050 (Bio-Rad Laboratories Inc.) for 95 min in an ice bath at 4˚C. After transfer, the membranes were blocked with 5% skimmed milk for 2 h (5% skimmed milk prepared in TBST containing 0.1% Tween 20). The blocked membranes were then incubated in a primary antibody solution at 4˚C overnight. After the first antibody incubation, the membrane was washed with TBST three times for 10 min each. Subsequently, the membrane was incubated with the secondary antibody at room temperature for 2 h. Finally, protein detection was performed using an enhanced chemiluminescence kit.

Reverse transcription-quantitative PCR (RT-qPCR). Total RNA from all the aforementioned cell lines was extracted with TRIzol® (Invitrogen; Thermo Fisher Scientific, Inc.), and cDNA synthesis was performed using a reverse transcription kit (cat. no. 1708891; Bio-Rad Laboratories, Inc.) according to the manufacturer's instructions. Next, iTaq™ Universal SYBR-Green Supermix (Bio-Rad Laboratories, Inc.) was added according to the qPCR reaction system, the reaction was centrifuged for a short time (5,000 x g, 4˚C, 10 sec) and then placed in an ABI 7500 (Applied Biosystems; Thermo Fisher Scientific, Inc.) fluorescent instrument for qPCR. The qPCR thermal cycling conditions consisted of an initial denaturation

step at 95C for 30 sec, followed by an annealing step at 95˚C for 15 sec and an extension step at 60˚C for 60 sec. The entire cycling process was repeated for a total of 40 cycles. The relative expression levels of LRP1 and CD36 mRNA were evaluated using the $2^{-\Delta\Delta Cq}$ method and normalized to β-actin (17). Primer sequences are listed in Table I.

Lentiviral transduction. Lentiviral short hairpin RNA LRP1 (LV-shLRP1) and lentiviral short-hairpin RNA negative control (LV-shNC) were made by and purchased from Shanghai GeneChem Co., Ltd. LV-shLRP1 transfections were performed to interfere with LRP1 expression in HGC-27, HepG2 and BxPC-3 cells according to manufacturer's instructions of the lentivirus. A total of 5,000 cells/well were seeded into a 6-well plate, with a multiplicity of infection of 10. The lentivirus concentration was $1x10^7$ TU/ml, and 10 μl lentivirus was added to each well. The transduction was performed at 37˚C in a 5% CO_2 incubator for 48 h. After 48 h, the cells were selected with 2 μl puromycin and maintained at a concentration of 500 μg/ml for 24 h. The medium was then changed, and the transfection efficiency was determined by observing green fluorescence. The efficiency of transfection was verified by western blotting. shRNA sequences are listed in Table II.

Cytotoxicity and proliferation assay. Cell proliferation was quantified using Cell Counting Kit-8 (CCK-8; Beyotime Institute of Biotechnology) according to manufacturer's instructions. CCK-8 reagent was applied for 2 h at 37˚C. The absorbance was measured at 450 nm with a microplate reader (Model 680; Bio-Rad Laboratories, Inc.), and values were calculated as an optical density index to compare proliferation before and after LRP1 knockdown. EdU staining was conducted using BeyoClick™ EdU Cell Proliferation kit with Alexa Fluor 594 (cat. no. C0078S; Beyotime Institute of Biotechnology) according to the manufacturer's instructions. Cells were observed under a fluorescence microscope (IX71; Olympus Corporation).

Colony formation assay. Cells infected with LV-shLRP1 and LV-shNC were transferred to a 6-well plate at a density of 1,000 cells/well. shNC- and shLRP1-infected cells were seeded in a 6-well plate and cultured at 37˚C for 15 days. Colonies were fixed at room temperature with glutaraldehyde (6.0% v/v) for 10 min, stained at room temperature with crystal violet (0.5% w/v) for 15 min before observation and images captured (Nikon D850 DSLR camera mounted on a Nikon TS2R-FL fluorescence microscope; Nikon Corporation; magnification, x40.).

Transwell assay. A Transwell assay was performed using Transwell membranes precoated with Matrigel (at 4˚C, then at 37˚C for 30 min), in accordance with the instructions of the Transwell assay kit (cat. no. 4322; Corning, Inc.). For cell resuspension (10,000 cells), 200 μl serum-free medium (DMEM; Gibco; Thermo Fisher Scientific, Inc.) containing 5% BSA (cat. no. ST023; Beyotime Institute of Biotechnology) was added to the upper chamber of Transwell; 500 μl medium containing 20% FBS was added to the lower chamber, and then cells were incubated at 37˚C in a 5% CO_2 cell incubator for 12-48 h. The Transwell plate culture medium was discarded, and the cells were fixed with 4% paraformaldehyde for 15 min and stained with 1 ml crystal violet for 10 min, both at room temperature. DAPI staining was also performed at room temperature in the dark for 5 min. The cells were observed under a fluorescence microscope (x200 magnification; Nikon Corporation).

Table I. Primer sequences for reverse transcription-quantitative PCR.

Gene	Primer sequence
Low-density lipoprotein receptor-related protein 1	Forward: 5'TAATCCCTCTGCTGTTGCTGC-3' Reverse: 5'-GGTTTCCAATCTCCACGTTCA-3'
CD36	Forward: 5'- GGAACTGTGGGCTCAT-3' Reverse: 5'- AGAATACCTCCAAACAC -3'
β-actin	Forward: 5'-CATGTACGTTGCTATCCAGGC-3'; Reverse: 5'-CTCCTTAATGTCACGCAGGAT-3'

Wound healing assay. For the wound healing assay, HGC-27 cells, HepG2 cells and BxPC-3 cells ($5x10^4$) were cultured in a 6-well plate until confluent (80%), then scratched with a 200-μl micropipette tip. The medium was replaced with fresh serum-free medium containing 10% FBS every 12 h. The wound healing area was measured at 0 and 48 h at 37˚C using a light microscope (x40 magnification; Nikon Corporation). The wound healing rate (%)=[(average wound area at 0 h/average wound area at 48 h/average wound area at 0 h] x100, and the relative wound healing rate (%) between shLRP1 group and shNC group was calculated with the shNC group as the control.

Hematoxylin and eosin (H&E) staining and immunohistochemistry. Paraffin sections (five sections each of gastric, liver and pancreatic cancer, and adjacent normal tissues were used as normal controls) were obtained from The Second Affiliated Hospital of Zhejiang University School of Medicine (Hangzhou, China). The paraffin section preparation process was as follows: All tissues (gastric, liver and pancreatic cancer, and cancer-adjacent tissues located 2 cm away from the lesion) were fixed in a 4% paraformaldehyde solution at room temperature for 48 h. Subsequently, they were dehydrated in a series of alcohol solutions with increasing concentrations at room temperature (50, 60, 70, 80 and 90% ethanol for 1 h each, 95% ethanol I for 1 h and 95% ethanol II for 1 h). After that, they were placed in a xylene-anhydrous ethanol mixture (1:1) for 30 min, xylene I for 10 min and xylene II for 5 min for clearing. The dehydrated and cleared tissues were then immersed in paraffin for 2 h at 60˚C. Once paraffin embedding was completed using an embedding machine, the tissue blocks were sectioned into 2-μm slices using a microtome and baked on a hot plate at 60˚C for 24 h. During H&E staining, the paraffin sections were subjected to deparaffinization and

Table II. shRNA sequences.

shRNA	Primer	Sequence
shLRP1	Sense primer	5'-GCAGTTTGCCTGCAGAGAT-3'
	Antisense primer	5'-ATCTCTGCAGGCAAACTGC-3'
shNC	Sense primer	5'-TTCTCCGAACGTGTCACGT-3'
	Antisense primer	5'-ACGTGACACGTTCGGAGAA-3'

shRNA, short hairpin RNA; LRP1, low-density lipoprotein receptor-related protein 1; NC, negative control.

hydration processes. The sections were sequentially immersed in two xylene solutions for 10 min each at room temperature, followed by immersion in 95, 85 and 70% ethanol for 5 min each to achieve full hydration. After hydration, the sections were rinsed with running water for 10 min. Subsequently, the sections were stained with hematoxylin for 10 min at room temperature, followed by 3 min of staining with 0.5% eosin at room temperature. After staining, the sections were dehydrated by immersing in 80% ethanol for 5 sec, 95% ethanol for 2 min and absolute ethanol for 2 min. The dehydrated tissue sections were then immersed in xylene twice, for 4 min each. Finally, the sections were air-dried and mounted with neutral mounting medium. The mounted slides were observed under a light microscope (x200 magnification; Nikon Corporation). Immunohistochemical analysis was performed using Histostain-streptavidin-peroxidase kit (cat. no. SP-0022; BIOSS) according to the manufacturer's instructions. Immunohistochemistry staining for the aforementioned paraffin sections was performed as follows: The fixed, deparaffinized, sectioned and baked sections were subjected to the same procedures as aforementioned. After hydration, the sections were placed in 50 ml citrate antigen retrieval solution (cat. no. P0081; Beyotime Institute of Biotechnology) and boiled at 100˚C for 10 min. After natural cooling, the sections were washed twice with distilled water for 5 min each. Subsequently, each section was incubated with 200 μl enhanced endogenous peroxidase blocking buffer (cat. no. P0100B; Beyotime Institute of Biotechnology) at room temperature for 20 min. Next, 100 μl of the primary antibody was added to cover each section, and the slides were incubated overnight at 4˚C. After washing three times with PBS for 5 min each, 100 μl HRP-labeled secondary antibody was added, and the slides were incubated at room temperature for 2 h. Finally, the sections were stained using the DAB Horseradish Peroxidase Color Development Kit (cat. no. P0203; Beyotime Institute of Biotechnology). The following primary antibodies were used for immunohistochemistry: LRP1 (cat. no. ab92544; 1:100; Abcam), CD36 (cat. no. ab252922; 1:100; Abcam) and horseradish peroxidase-conjugated goat-anti-mouse secondary antibody (cat. no. GAM007; 1:100; Multi Sciences Biotech Co,. Ltd.). The slides were observed under a light microscope (BX41; Olympus Corporation) at x200 magnification.

Oil Red O staining. A total of 5x10^5 cells/well (HGC-27, HepG2 and BxPC-3 cells transfected with shNC and shLRP1) were inoculated in a 6-well plate. After 24 h of culture (at 37˚C in a 5% CO_2 humidified incubator), the culture medium (HGC-27 cells and BxPC-3 cells were cultured in RPMI-1640 medium, while HepG2 cells were cultured in DMEM) was discarded. Following fixation with 4% paraformaldehyde for 15 min, Oil Red O staining was performed for 15-20 min, both at room temperature. Decolorization (at room temperature for 5 min) with 60% isopropanol was performed to remove excess dye. Slides were subsequently observed under a light microscope (BX41; Olympus Corporation) at x200 magnification.

Statistical analysis. Statistical analysis was performed using SPSS (version 19.0; IBM Corp.), R (version 3.6.3; r-project.org/) and GraphPad Prism (version 9.3.0; Dotmatics). Groups with multiple tumor subtypes were compared using Wilcoxon rank-sum test. Survival analysis was performed using the Kaplan-Meier method, and log-rank test was used for comparing survival times. Cox proportional hazards model was employed for univariate and multivariate analysis to identify prognostic factors. Pearson correlation coefficient was used to examine the correlation between LRP1 gene and gastric, liver and pancreatic cancer. Data were normalized using the Z-score standardization method. Wound healing and invasion assays were analyzed using a two-tailed unpaired Student's t-test for two-group comparisons. One-way ANOVA followed by Tukey's post hoc test was used to assess the differences in mRNA and protein expression among >2 groups. Data are presented as the mean ± standard deviation of ≥3 independent experimental repeats. $P<0.05$ was considered to indicate a statistically significant difference.

Results

High expression of LRP1 predicts poor prognosis in GI tumors. The expression of LRP1 in tumor tissue was evaluated using TCGA database and the GTEx project. LRP1 was expressed at higher levels in tumor compared with the corresponding normal tissues (Fig. 1A), including adrenocortical, bladder urothelial, breast invasive and cervical squamous cell carcinoma and endocervical adenocarcinoma, cholangiocarcinoma, colon adenocarcinoma (COAD), lymphoid neoplasm diffuse large B cell lymphoma, esophageal carcinoma, glioblastoma multiforme, head and neck squamous cell carcinoma, kidney chromophobe and renal clear and papillary cell carcinoma, acute myeloid leukemia, brain lower grade glioma, liver hepatocellular carcinoma (LIHC), lung adenocarcinoma and squamous cell carcinoma, ovarian serous cystadenocarcinoma, pancreatic adenocarcinoma (PAAD), pheochromocytoma and paraganglioma and prostate, rectum

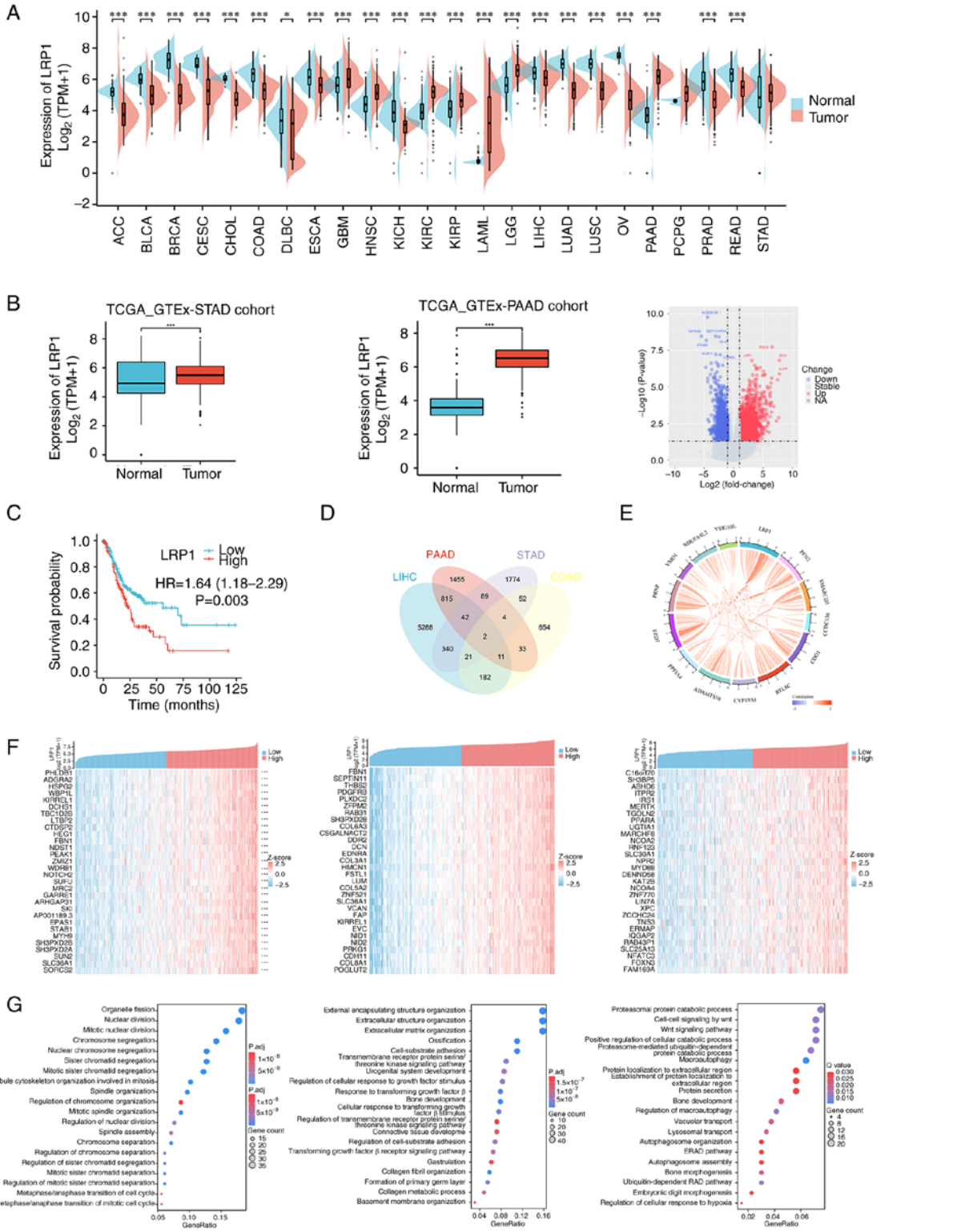

Figure 1. High expression of LRP1 is associated with poor prognosis in gastrointestinal tumor. (A) LRP1 expression profile in various cancers and normal specimens. (B) LRP1 expression in tumor and normal tissues in STAD and PAAD from TCGA database. (C) Correlation between LRP1 and prognosis of STAD. (D) Prognosis-associated genes of STAD, PAAD, COAD and LIHC, and (E) their correlation with LRP1. (F) Top 30 genes positively associated with LRP1 shown in heatmap. (G) Significant Gene Ontology terms of the top 300 genes positively associated with LRP1, including cell proliferation pathway in STAD (left image), extracellular matrix formation and regulation of transmembrane receptor proteins pathways in PAAD (middle image), extracellular matrix formation and regulatory pathways of transmembrane receptor proteins in LIHC (right image). The statistical method used for GOKEGG enrichment analysis is Fisher's exact test, with a P-value <0.05 and FDR=0.05. *P<0.05, ***P<0.001 vs. normal. LRP1, low-density lipoprotein receptor-related protein 1; STAD, stomach adenocarcinoma; PAAD, pancreatic adenocarcinoma; TCGA, The Cancer Genome Atlas; GTEx, Genotype-Tissue Expression; HR, hazard ratio; TPM, transcripts per million; NA, not available; ACC, adrenocortical carcinoma; BLCA, bladder urothelial carcinoma; BRCA, breast invasive carcinoma; CESC, cervical and endocervical cancers; CHOL, cholangiocarcinoma; COAD, colon adenocarcinoma; DLBC, diffuse large B-cell lymphoma; ESCA, esophageal carcinoma; GBM, glioblastoma multiforme; HNSC, head and neck squamous cell carcinoma; KICH, kidney chromophobe; KIRC, kidney renal clear cell carcinoma; KIRP, kidney renal papillary cell carcinoma; LAML, acute myeloid leukemia; LGG, lower grade glioma; LIHC, liver hepatocellular carcinoma; LUAD, lung adenocarcinoma; LUSC, lung squamous cell carcinoma; OV, ovarian serous cystadenocarcinoma; PCPG, pheochromocytoma and paraganglioma; PRAD, prostate adenocarcinoma; READ, rectum adenocarcinoma.

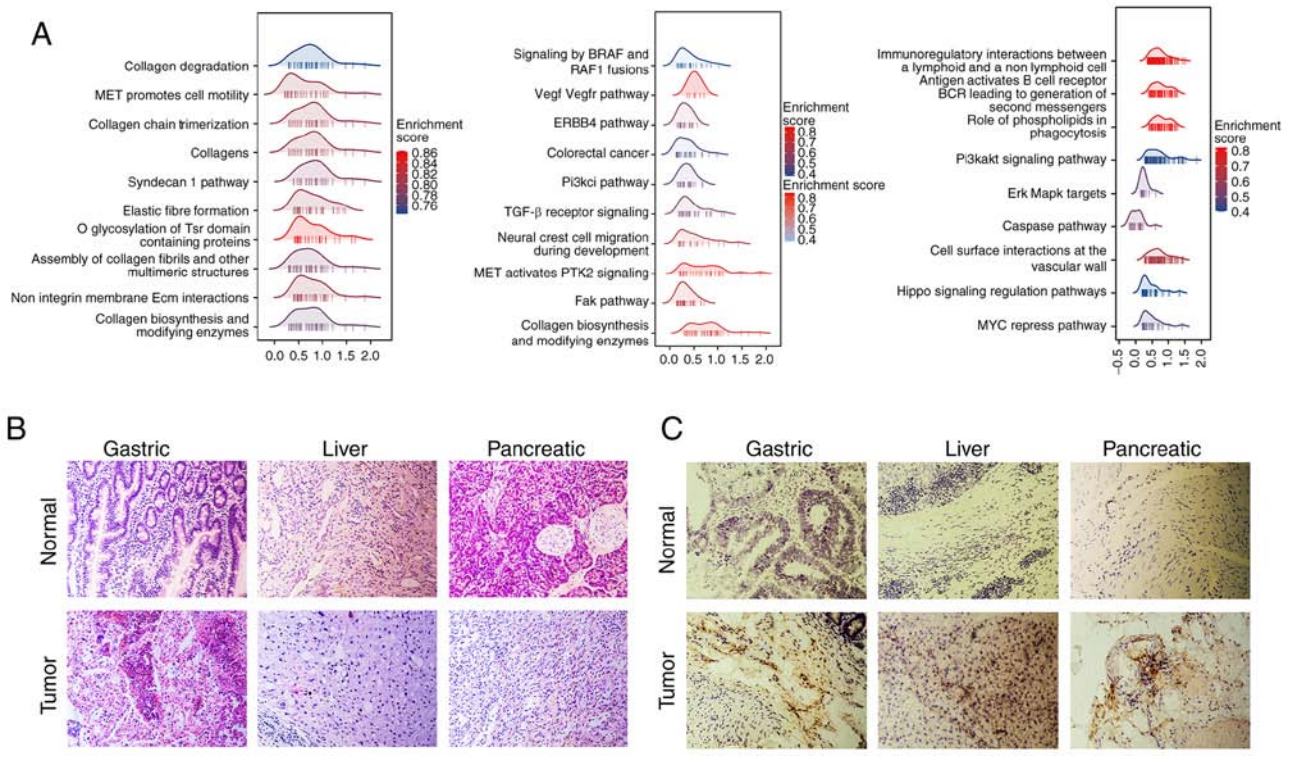

Figure 2. Differential analysis and GSEA of LRP1. (A) Significant GSEA results of LRP1. (B) Human gastric, liver and pancreatic cancer and normal tissues stained with hematoxylin and eosin. (C) Gastric, liver and pancreatic cancer tissue were immunochemically stained using LRP1 (brown). Magnification, x200. GSEA, gene set enrichment analysis; LRP1, low-density lipoprotein receptor-related protein 1.

and stomach adenocarcinoma (STAD). Furthermore, in TCGA database, expression of LRP1 was higher in STAD and PAAD tissues compared with that in adjacent normal tissue. Differential gene analysis of the pancreatic cancer data in TCGA database showed that LRP1 was significantly upregulated in PAAD [P<0.05; log fold-change (FC)>5; Fig. 1B]. These results suggested that LRP1 may play a key role in the pathogenesis of GI tumors. To evaluate the effect of LRP1 expression in predicting the prognosis of patients with GI cancer, the association between LRP1 expression and overall survival in STAD was analyzed (Fig. 1C). High LRP1 expression was associated with poor prognosis in STAD (P=0.003). Cox's regression test was used to analyze prognosis-associated genes in PAAD, STAD, COAD and LIHC. The expression of the top 13 prognosis-associated genes in STAD, COAD and LIHC (Fig. 1D) was positively correlated with LRP1 expression in pancreatic cancer (specifically PAAD) (Fig. 1E).

To explore the function and pathways of LRP1 in GI tumors, correlation analysis between LRP1 and other mRNAs in STAD, PAAD and LIHC was performed using TCGA. The top 30 genes that were positively correlated with LRP1 expression were visualized as a heatmap (Fig. 1F). R software package 'clusterProfiler' was used to explore the potential functions and pathways of the top 300 correlated genes. GO functional enrichment analysis showed that in STAD, LRP1 was primarily associated with pathways associated with cell proliferation, including 'mitotic nuclear division' and 'microtubule cytoskeleton organization involved in mitosis'. In PAAD, LRP1 was primarily associated with pathways such as 'extracellular matrix organization' and 'transmembrane receptor protein serine/threonine kinase signaling pathway'. In LIHC, LRP1 was primarily associated with pathways associated with protein metabolism ('proteasomal protein catabolic process'), 'Wnt signaling pathway' and autophagy ('autophagosome organization' and 'autophagosome assembly') (Fig. 1G). These results suggested that high expression of LRP1 in PAAD, STAD and LIHC may be a result of upregulation of multiple pathways associated with cancer formation in GI tumors, particularly those that control cell proliferation and metastasis.

Differential and Gene Set Enrichment Analysis (GSEA) of LRP1. Differential expression and correlation analysis was performed to analyze the potential effects of LRP1 upregulation in GI tumors. R package 'DESeq2' was used to analyze the differential expression of LRP1 in STAD, PAAD and LIHC, and GSEA was performed on the top 30 genes with log(FC)>0. Differentially expressed genes in all the three cancer types were significantly enriched in pathways that promote cancer occurrence and development, such as MET and ERK, and other pathways (Fig. 2A; 'collagen chain trimerization', 'assembly of collagen fibrils and other multimeric structures' and 'fak pathway') that regulate collagen production and degradation (Fig. 2A).

H&E staining showed the difference between normal and tumor tissues. Compared with the normal tissues, the tissue samples from gastric, pancreatic and liver cancer exhibited structural disorganization, disarrayed cell arrangements, increased cell density and thickening of the extracellular matrix (Fig. 2B). Immunohistochemical experiments were conducted to compare the differences in LRP1 expression between normal and tumor GI tissue. Immunohistochemistry showed that expression of LRP1 was upregulated in GI cancer compared with that in normal tissues (Fig. 2B and C).

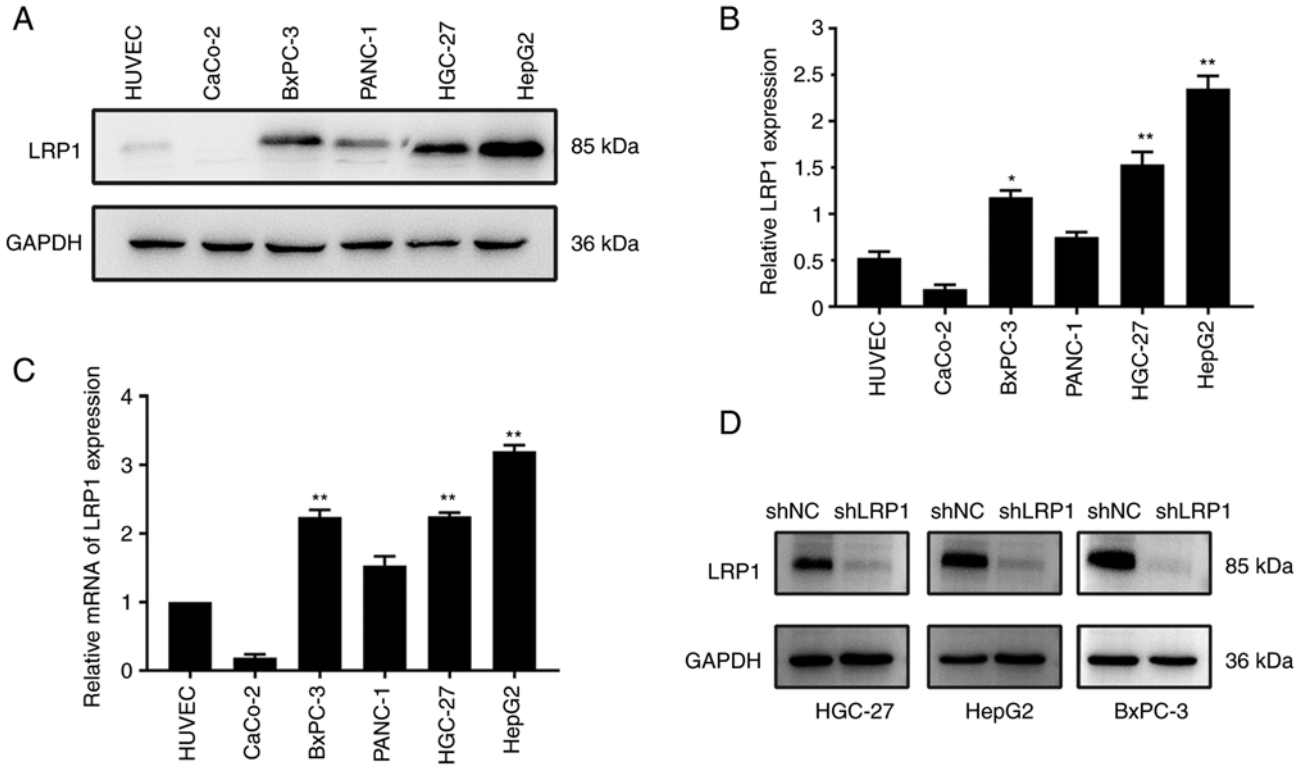

Figure 3. LRP1 is expressed at high levels in HGC-27, HepG2 and BxPC-3 cells. (A) Expression of LRP1 and loading control GAPDH in HUVEC, CaCo-2, BxPC-3, PANC-1, HGC-27 and HepG2 cells was investigated by western blotting. (B) Relative expression of LRP1 in HUVEC, CaCo-2, BxPC-3, PANC-1, HGC-27 and HepG2 cells. (C) Expression of LRP1 gene in HUVEC, CaCo-2, BxPC-3, PANC-1, HGC-27 and HepG2 cells was investigated by quantitative PCR. (D) Expression of LRP1 and loading control GAPDH in HGC-27, HepG2 and BxPC-3 cells before and after lentiviral transfection was investigated by western blotting. *P<0.05, **P<0.01 vs. HUVEC. LRP1, low-density lipoprotein receptor-related protein 1; shNC, short hairpin negative control. Unpaired Student's t-test was used for analysis.

LRP1 is expressed at high levels in HGC-27, HepG2 and BxPC-3 cells. The expression of LRP1 in gastric HGC-27, liver HepG2 cells and pancreatic BxPC-3 cancer cells was notably increased compared with that in HUVECs (Fig. 3A). Protein expression of LRP1 was significantly higher in BxPC-3 compared with in HUVECs (P<0.05). Protein expression of LRP1 was also significantly higher in HGC-27 and HepG2 cells compared with that in control HUVECs (P<0.01; Fig. 3B). The mRNA expression of LRP1 in HGC-27, HepG2 and BxPC-3 cells was significantly higher than that in HUVECs (P<0.01; Fig. 3C). To investigate the effect of LRP1 on GI cancer cells, LRP1 was knocked down via transfection of HGC-27, HepG2 and BxPC-3 cells with LV-shLPR1 (Fig. S1B). Western blotting showed that LRP1 protein expression levels in cells in which LRP1 was knocked down were decreased compared with those in cells transfected with shNC (Fig. 3D). Quantitative analysis is shown in Fig. S1A. Transfection efficiency was ≥80% for shNC and shLRP1 in HGC-27, HepG2 and BxPC-3 cells (Fig. S1B). Based on the findings from the bioinformatics analysis and experimental results (Fig. 3A), it was observed that LRP1 exhibits low expression levels in both normal tissues and cells. Consequently, it was hypothesized that attempting to further suppress LRP1 in cells that already possess a baseline low expression would not result in significant effects.

Decreased LRP1 expression can inhibit the proliferation of GI tumor cells. To investigate the effect of LRP1 knockdown on proliferation of GI cancer cells, CCK-8 and EdU cell proliferation assays were performed on HGC-27, HepG2 and BxPC-3 cells following transfection. CCK-8 assay showed that cell proliferation was decreased after transfection with LV-shLRP1 (Fig. 4A-C). EdU proliferation assay showed that the proliferation of HGC-27, HepG2 and BxPC-3 cells was inhibited and the number of dividing cells decreased after LRP1 knockdown (Fig. 4D).

Western blotting showed that expression of p-AKT and EGFR proteins in HGC-27, HepG2 and BxPC-3 cells was inhibited following knockdown of LRP1 (Fig. 4E). The aforementioned data showed that the proliferation of HGC-27, HepG2and BxPC-3 cells was inhibited after LRP1 knockdown.

Decreased LRP1 expression can inhibit the invasion and migration of GI cancer cells. To investigate whether LRP1 is related to the invasion and migration of GI cancer cells, Transwell and wound healing assays were performed; invasion and migration ability of HGC-27, HepG2 and BxPC-3 cells decreased following LRP1 knockdown. Compared with cells transfected with shNC, invasion of HGC-27, HepG2 and BxPC-3 cells was reduced after LRP1 knockdown (Fig. 5A). Wound healing assay confirmed that the migration of GI tumor cells was decreased following LRP1 knockdown (Fig. 5B). Based on preliminary investigations, it was determined that 48 h post-transfection gave the optimal efficiency of lentiviral transduction. Compared with cells transfected with shNC, colony formation assay demonstrated that LRP1 knockdown effectively suppressed cell proliferation (Fig. 5C). Western blotting showed that

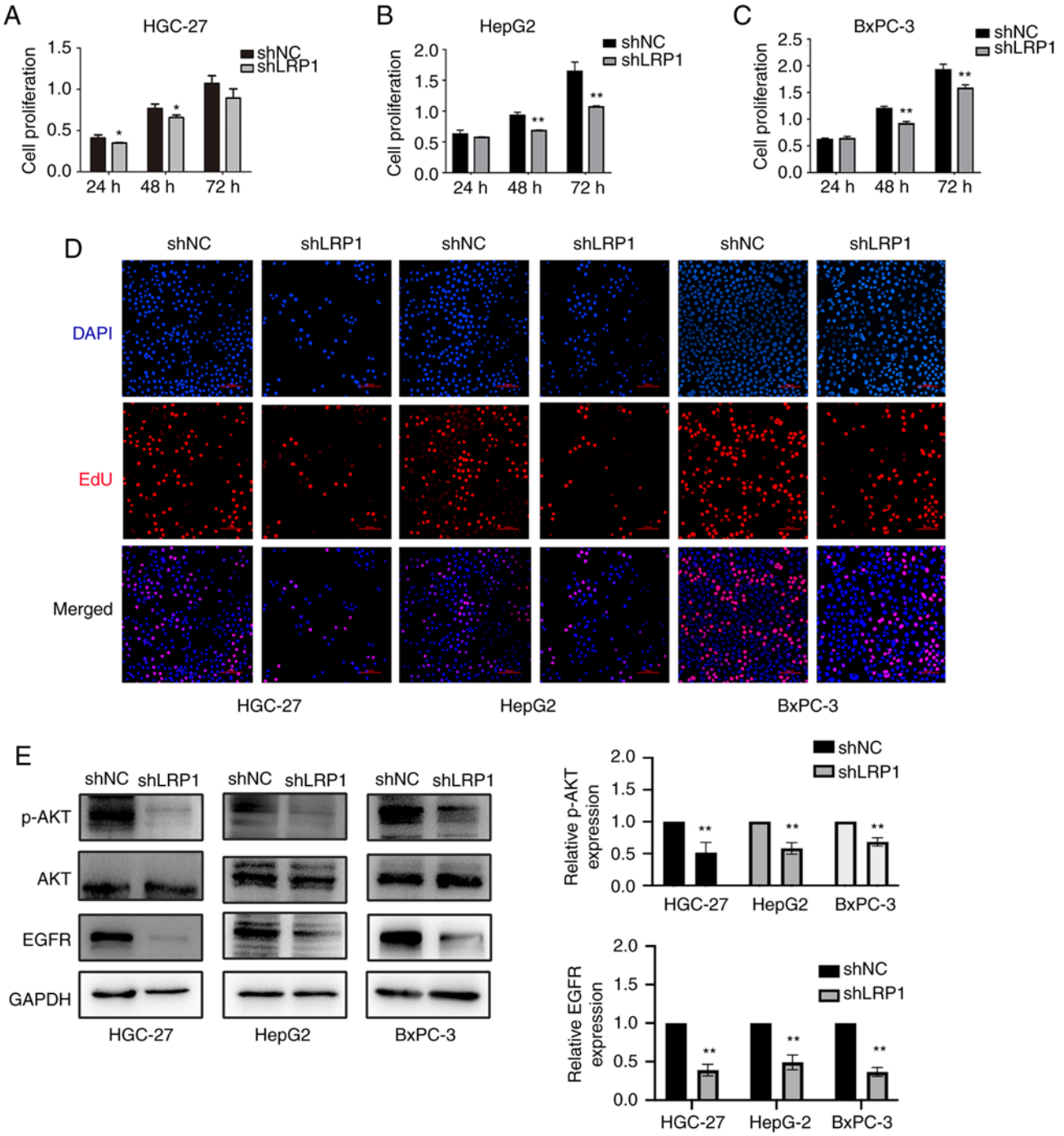

Figure 4. Decreased LRP1 expression could inhibit the proliferation of gastrointestinal tumor cells. Relative proliferation of (A) HGC-27, (B) HepG2 and (C) BxPC-3 cells was determined using Cell-Counting Kit 8. (D) EdU cell proliferation experiment. Magnification, x200. (E) Expression of p-AKT, AKT and EGFR and loading control GAPDH in HGC-27, HepG2 and BxPC-3 cells before and after lentiviral transfection was examined by western blotting. *P<0.05 and **P<0.01 vs. shNC. p, phosphorylated; EGFR, epidermal growth factor receptor; LRP1, low-density lipoprotein receptor-related protein 1; shNC, short hairpin negative control. Unpaired Student's t-test was used for analysis.

protein expression of p-ERK and MMP-9 in HGC-27, HepG2 and BxPC-3 cells was significantly downregulated following LRP1 knockdown. Expression of ERK and MMP-2 proteins in BxPC-3 cells decreased significantly (Fig. 5D).

Decreased LRP1 expression can inhibit lipid absorption. Lipid metabolism is mainly accomplished via the digestive system (18). To explore the impact of LRP1 knockdown on lipid metabolism in GI tumor cells, the expression of related genes (LRP1 and CD36) was detected via qPCR. LRP1 gene expression was significantly downregulated in HGC-27, HepG2 and BxPC-3 cells following LRP1 knockdown compared with that in cells transfected with shNC (Fig. 6A). CD36 gene expression in HepG2 and BxPC-3 cells was significantly downregulated after LRP1 knockdown compared with that in cells transfected with shNC (P<0.01; Fig. 6B). Oil Red O staining showed that lipids accumulated in GI tumor cells after LRP1 knockdown (Fig. 6C). CD36 is a scavenger receptor responsible for the

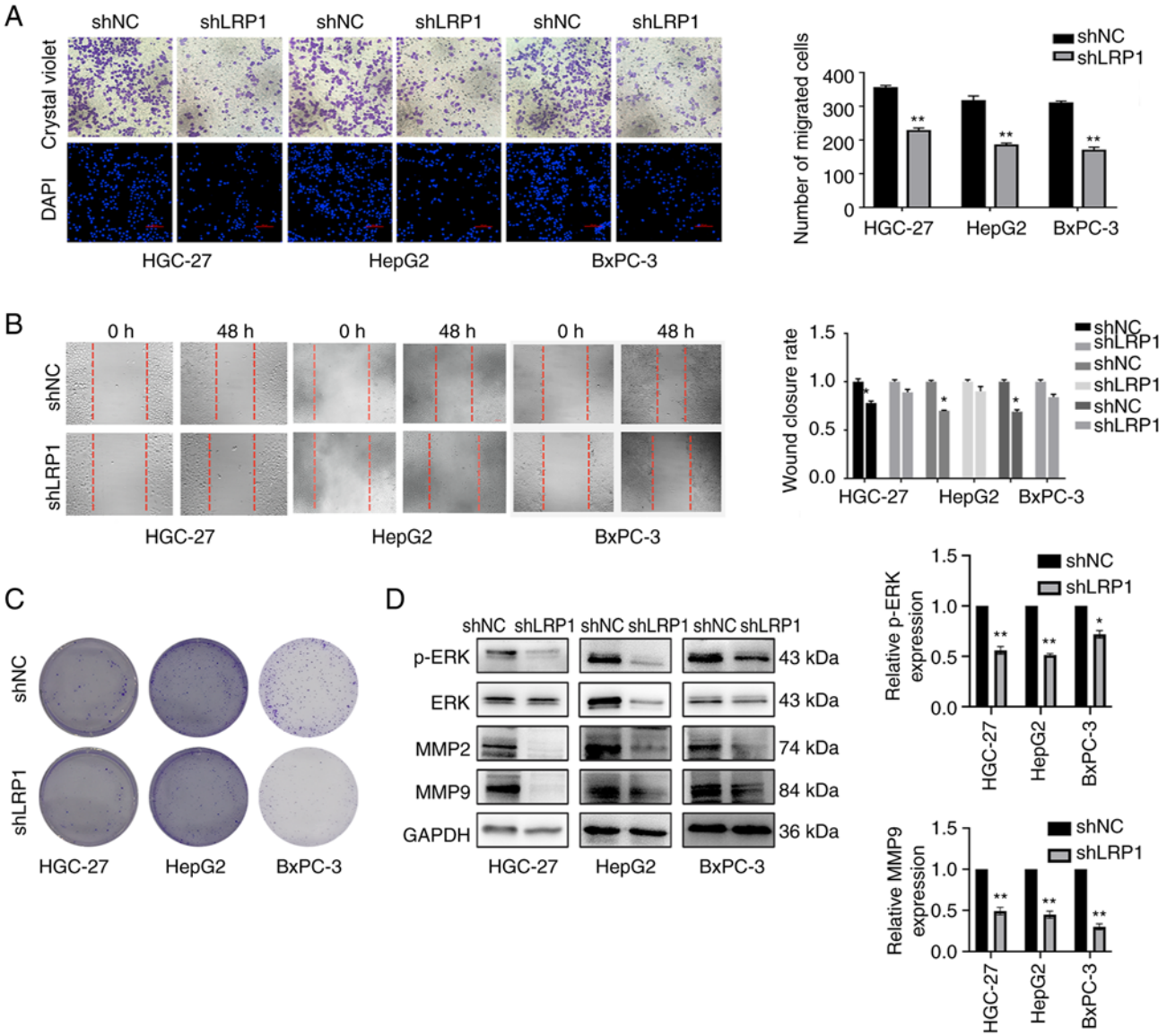

Figure 5. Decreased LRP1 expression inhibits invasion and migration of gastrointestinal tumor cells. (A) Transwell assay of HGC-27 cells, HepG2 cells and BxPC-3 cells before and after lentivirus transfection. Magnification, x200. (B) Wound healing assay of HGC-27, HepG2 and BxPC-3 cells before and after lentivirus transfection. Magnification, x100. (C) Colony formation before and after lentivirus transfection of HGC-27 cells, HepG2 cells and BxPC-3 cells. Magnification, x40. (D) Expression of p-ERK, ERK, MMP-2, MMP-9 and loading control GAPDH in HGC-27, HepG2 and BxPC-3 cells before and after lentivirus transfection was investigated by western blotting. *P<0.05 and **P<0.01 vs. shNC. p, phosphorylated; LRP1, low-density lipoprotein receptor-related protein 1; shNC, short hairpin negative control. Unpaired Student's t-test was used for analysis.

uptake/transport of lipids and oxidized LDL (19). CD36 was upregulated in liver and pancreatic cancer tissues compared with that in normal GI tissue (Fig. 6D). These results suggested that LRP1 knockdown inhibited lipid absorption of GI tumors.

Discussion

In recent years, the incidence of GI cancers has increased worldwide. The stage at diagnosis of GI cancer is closely associated with the survival rate; early stage detection could reduce the mortality rate. However, there are no specific symptoms characterizing early stage of GI cancers; due to its insidious onset and deep anatomical location, diagnosis of early-stage GI cancer is challenging (20). Although biomarkers such as CA19-9 (21) and CA-125 (22) are available, the association between these indicators and tumor metastasis, invasion or prognosis remains unclear. Therefore, it is important to find an effective therapeutic target and novel biomarkers. Based on bioinformatics analysis, high expression of LRP1 was associated with poor prognosis in GI tumor in the present study. It was found that LRP1 was expressed at high levels in GI cancer cell lines HGC-27, HepG2 and BxPC-3, and the knockdown of LRP1 changed the biological characteristics (cell proliferation, invasion, migration and viability) of the GI tumor cells. The knockdown of LRP1 could inhibit the proliferation of GI tumor cells. EdU cell proliferation experiments showed that compared with the control (shNC) group, proliferation of gastric (HGC-27), liver (HepG2) and pancreatic (BxPC-3) cancer cells was suppressed following LRP1 knockdown. In addition, cell population dependence increased after LRP1 knockdown, which inhibited the formation of cell clones. To elucidate the mechanism by which LRP1 knockdown could

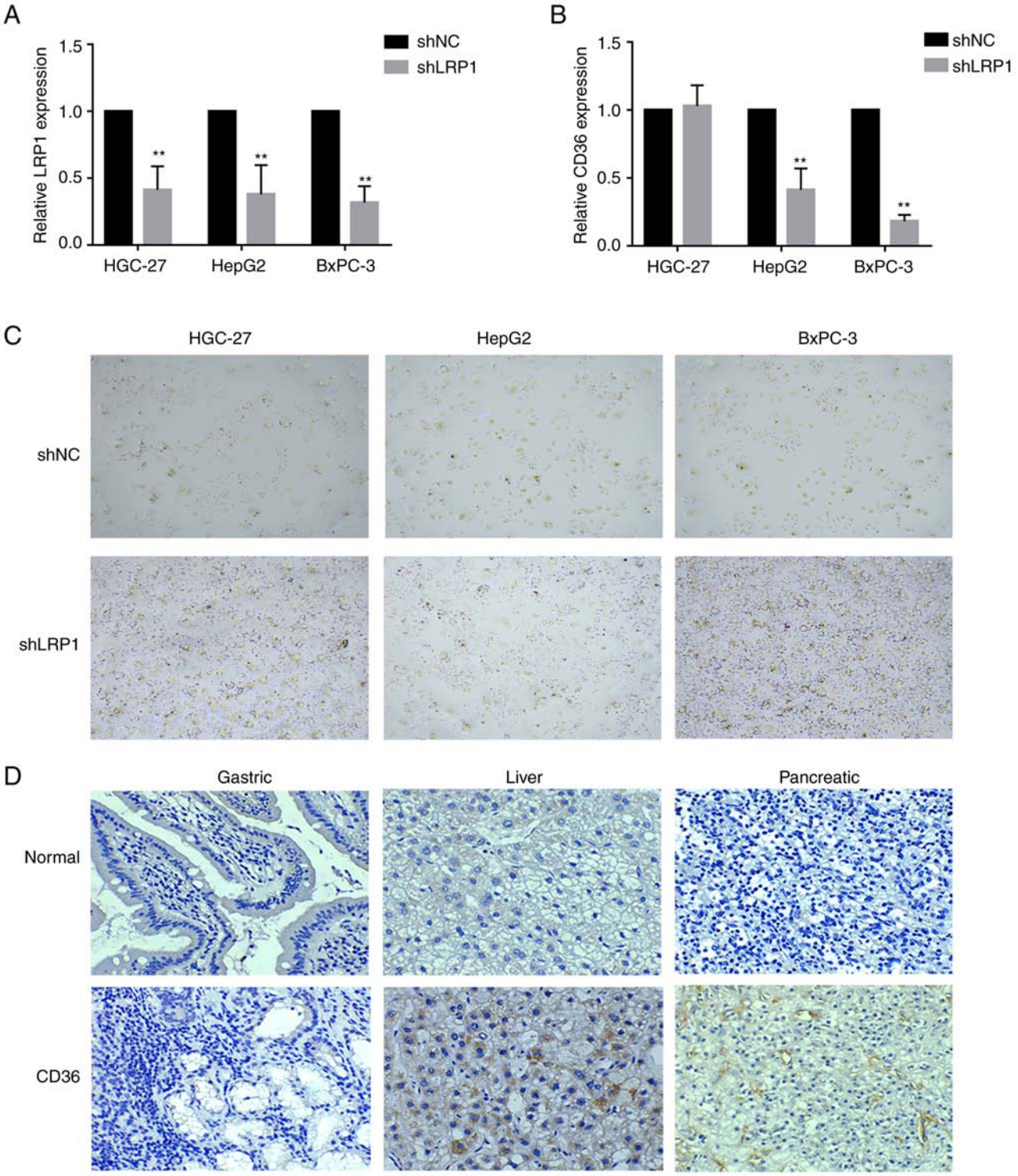

Figure 6. Decreased LRP1 expression inhibits lipid absorption. Expression of (A) LRP1 and (B) CD36 in HGC-27, HepG2 and BxPC-3 cells before and after LV-shLRP1 transfection was examined by quantitative PCR. **P<0.01 vs shNC. (C) Lipid (red) accumulation in HGC-27, HepG2 and BxPC-3 cells detected by Oil Red O staining. Magnification, x200. (D) Gastric, liver and pancreatic cancer tissue was immunochemically stained using CD36 (brown) antibodies. Magnification, x200. Unpaired Student's t test was used for analysis. LRP1, low-density lipoprotein receptor-related protein 1; shNC, short hairpin-negative control.

inhibit the proliferation of GI tumor cells, AKT and EGFR protein expression was measured using western blotting. LRP1 knockdown inhibited phosphorylation of AKT and the expression of EGFR protein (Fig. 3E). AKT is a key survival signal transduction protein and it is a downstream target of EGFR (23). MMP2 and MMP9 are proteases associated with tumor invasion and migration (24). LRP1-mediated regulation of MMP expression promotes cancer cell migration and invasion (25). LRP1 serves as an endocytic receptor for MMP2 and MMP9, thus regulating tumor invasion and migration (25). A previous study (1) demonstrated that LRP1 induces protein expression of MMP2 and MMP9, thereby

promoting migration and invasion of human glioblastoma U87 cells. In the present study, expression of MMP2 and MMP9 was selectively decreased in cells following LRP1 knockdown. p-ERK in LRP1-knockdown cells was also significantly decreased, which suggested that LRP1 regulates MMP2 and MMP9 via the ERK signaling pathway (26). In the present study, the expression of p-ERK, MMP2 and MMP9 was reduced. Transwell and wound healing assay showed that the invasion and migration of HGC-27, HepG2 and BxPC-3 cells were decreased compared with those in the control group. The ERK signaling pathway transmits extracellular stimuli to the nucleus and regulates tumorigenesis, proliferation, apoptosis and drug resistance (27,28). Decreased LRP1 expression inhibited the proliferation, invasion and migration of GI tumor cells. Tumor cells have a strong metabolism to grow rapidly, especially the digestive tract cells which are involved in digestion and absorption of nutrients. Compared with normal cells, tumor cells possess enhanced metabolic capacity and exhibit accelerated growth. Therefore, we hypothesize that following the transformation of digestive tract cells involved in nutrient digestion and absorption to provide nutrients to cells, the metabolic and growth capabilities become more prominent. Compared with normal cells, cancer cells obtain more energy via lipid metabolism to promote cell proliferation, invasion and migration, which accounts for high expression of LRP1 in GI tumor cells (29). Moreover, inactivation of LRP1 in adipocytes could lead to delayed lipid clearance after a meal, change in adipocyte tissue metabolism, glucose tolerance and obesity resistance induced by a high-fat diet (30). In mouse intestinal polyps, the expression of LRP1 is ~3-fold higher than that in normal tissues (31). LRP1 is expressed at high levels in both human lung adenocarcinoma A549 and colorectal cancer cells (32). Another study found that lipid-associated metabolic pathways are activated at high levels in pancreatic cancer; LRP1 expression in pancreatic cancer is double that in normal pancreatic tissue (33). Blocking LRP1-mediated cholesterol endocytosis via LRP1 gene knockdown disrupts the homeostasis of cholesterol inside and outside the cell, affecting the proliferation and tumorigenicity of pancreatic cancer cells, and inhibits ERK-dependent survival pathways (34). Therefore, the expression of LRP1 may be associated with mediating the uptake of cholesterol in pancreatic cancer cells, consequently exerting further influence on the growth of tumor cells. Rohlmann *et al* (35) showed that LDLR partially compensates for the loss of LRP1 in hepatocytes and increased expression of LDLR indicates that LRP1 plays an important role in elimination of residual lipoproteins in the liver. In another study, plasma triglycerides in LRP1-deficient mice receiving normal diet increases by 2-fold. Under a high-fat diet, morphological examination and Oil Red O staining of liver sections show notable accumulation of lipid droplets in LRP1-deficient mice (36). In the present study, BxPC-3 cells had the most significant decrease in CD36 gene expression following LRP1 knockdown and Oil Red O staining showed that decreased LRP1 expression increased lipid accumulation in BxPC-3 cells. A previous study showed that relative expression levels of CD36 are important for lipid absorption in mammals (37). Thus, it was hypothesized that LRP1 affects cholesterol absorption in tumor cells by regulating expression of CD36. Here, LRP1 was expressed at high levels in BxPC-3, HGC-27 and HepG2 cells and high expression of LRP1 was associated with poor prognosis in GI tumors and increased proliferation of GI tumor cells. Knocking down expression of LRP1 may interfere with tumor cell lipid metabolism, resulting decreased EGFR, p-AKT, p-ERK proteins and membrane molecule CD36, MMP2 and MMP9 expression, thereby inhibiting metastasis and invasion of GI tumors. The present study demonstrated the regulatory role of LRP1 in invasion and prognosis of GI cancer and also suggested that LRP1 may be a novel target for the treatment of GI cancer.

Acknowledgements

Not applicable.

Funding

The present study was supported by the Natural Science Foundation of Zhejiang Province (grant nos. LY19H060001, LQ19H160044 and LGF21H160016).

Availability of data and materials

The datasets used and/or analyzed during the current study are available from the corresponding author on reasonable request.

Authors' contributions

MZ, HS, BW conceived and designed the study. HS and BW analyzed the data. MZ drafted the manuscript. YH, JC, JR, ZZ and XJ participated in the statistical analysis and had input in the experimental design. YH, JC, JR, ZZ and XJ confirm the authenticity of all the raw data. All authors have read and approved the final manuscript.

Ethics approval and consent to participate

The present study was approved by Institutional Animal Care and Use Committee (approval no. IACUC-20190429-09) and Medical Ethics Committee of Zhejiang Chinese Medical University (approval no. 20221011-5).

Patient consent for publication

Not applicable.

Competing interests

The authors declare that they have no competing interests.

References

1. Song H, Li Y, Lee J, Schwartz AL and Bu G: Low-density lipoprotein receptor-related protein 1 promotes cancer cell migration and invasion by inducing the expression of matrix metalloproteinases 2 and 9. Cancer Res 69: 879-886, 2009.
2. Cheng C, Geng F, Cheng X and Guo D: Lipid metabolism reprogramming and its potential targets in cancer. Cancer Commun (Lond) 38: 27, 2018.
3. Arnold M, Abnet CC, Neale RE, Vignat J, Giovannucci EL, McGlynn KA and Bray F: Global burden of 5 major types of gastrointestinal cancer. Gastroenterology 159: 335-349 e15, 2020.

4. Sung H, Ferlay J, Siegel RL, Laversanne M, Soerjomataram I, Jemal A and Bray F: Global cancer statistics 2020: GLOBOCAN estimates of incidence and mortality worldwide for 36 cancers in 185 countries. CA Cancer J Clin 71: 209-249, 2021
5. Malvicini M, Aquino JB and Mazzolini G: Combined therapy for gastrointestinal carcinomas: Exploiting synergies between gene therapy and classical chemo-radiotherapy. Curr Gene Ther 15: 151-160, 2015.
6. Xu Q, Zong L, Chen X, Jiang Z, Nan L, Li J, Duan W, Lei J, Zhang L, Ma J, *et al*: Resveratrol in the treatment of pancreatic cancer. Ann N Y Acad Sci 1348: 10-19, 2015.
7. Feng F, Tian Y, Xu G, Liu Z, Liu S, Zheng G, Guo M, Lian X, Fan D and Zhang H: Diagnostic and prognostic value of CEA, CA19-9, AFP and CA125 for early gastric cancer. BMC Cancer 17: 737, 2017.
8. Zhang L, Sanagapalli S and Stoita A: Challenges in diagnosis of pancreatic cancer. World J Gastroenterol 24: 2047-2060, 2018.
9. Wang B, Shen C, Li Y, Zhang T, Huang H, Ren J, Hu Z, Xu J and Xu B: Oridonin overcomes the gemcitabine resistant PANC-1/Gem cells by regulating GST pi and LRP/1 ERK/JNK signalling. Onco Targets Ther 12: 5751-5765, 2019.
10. Gheysarzadeh A, Ansari A, Emami MH, Razavi AE and Mofid MR: Over-expression of low-density lipoprotein receptor-related Protein-1 is associated with poor prognosis and invasion in pancreatic ductal adenocarcinoma. Pancreatology 19: 429-435, 2019.
11. Guillaumond F, Bidaut G, Ouaissi M, Servais S, Gouirand V, Olivares O, Lac S, Borge L, Roques J, Gayet O, *et al*: Cholesterol uptake disruption, in association with chemotherapy, is a promising combined metabolic therapy for pancreatic adenocarcinoma. Proc Natl Acad Sci USA 112: 2473-2478, 2015.
12. Gopal U, Bohonowych JE, Lema-Tome C, Liu A, Garrett-Mayer E, Wang B and Isaacs JS: A novel extracellular Hsp90 mediated co-receptor function for LRP1 regulates EphA2 dependent glioblastoma cell invasion. PLoS One 6: e17649, 2011.
13. Huang XY, Shi GM, Devbhandari RP, Ke AW, Wang Y, Wang XY, Wang Z, Shi YH, Xiao YS, Ding ZB, *et al*: Low level of low-density lipoprotein receptor-related protein 1 predicts an unfavorable prognosis of hepatocellular carcinoma after curative resection. PLoS One 7: e32775, 2012.
14. Vivian J, Rao AA, Nothaft FA, Ketchum C, Armstrong J, Novak A, Pfeil J, Narkizian J, Deran AD, Musselman-Brown A, *et al*: Toil enables reproducible, open source, big biomedical data analyses. Nat Biotechnol 35: 314-316, 2017.
15. Subramanian A, Tanayo P, Mootha VK, Mukherjee S, Ebert BL, Gillette MA, Paulovich A, Pomeroy SL, Golub TR, Lander ES and Mesirov JP: Gene set enrichment analysis: A knowledge-based approach for interpreting genome-wide expression profiles. Proc Natl Acad Sci USA 102: 15545-15550, 2005.
16. Mootha VK, Lindgren CM, Erlksson KF, Subramanian A, Sihag S, Lehar J, Puigserver P, Carlsson E, Ridderstråle M, Laurila E, *et al*: PGC-1alpha-responsive genes involved in oxidative phosphorylation are coordinately downregulated in human diabetes. Nat Genet 34: 267-273, 2003.
17. Livak KJ and Schmittgen TD: Analysis of relative gene expression data using real-time quantitative PCR and the 2(-Delta Delta C(T)) method. Methods 25: 402-408, 2001.
18. Font-Burgada J, Sun B and Karin M: Obesity and cancer: The oil that feeds the flame. Cell Metab 23: 48-62, 2016.
19. Wang J and Li Y: CD36 tango in cancer: Signaling pathways and functions. Theranostics 9: 4893-4908, 2019.
20. Necula L, Matei L, Dragu D, Neagu AI, Mambet C, Nedeianu S, Bleotu C, Diaconu CC and Chivu-Economescu M: Recent advances in gastric cancer early diagnosis. World J Gastroenterol 25: 2029-2044, 2019.
21. Wei X, Li YB, Li Y, Lin BC, Shen XM, Cui RL, Gu YJ, Gao M, Li YG and Zhang S: Prediction of lymph node metastases in gastric cancer by serum APE1 expression. J Cancer 8: 1492-1497, 2017.
22. Zang R, Li Y, Jin R, Wang X, Lei Y, Che Y, Lu Z, Mao S, Huang J, Liu C, *et al*: Enhancement of diagnostic performance in lung cancers by combining CEA and CA125 with autoantibodies detection. Oncoimmunology 8: e1625689, 2019.
23. Tiemin P, Fanzheng M, Peng X, Jihua H, Ruipeng S, Yaliang L, Yan W, Junlin X, Qingfu L, Zhefeng H, *et al*: MUC13 promotes intrahepatic cholangiocarcinoma progression via EGFR/PI3K/AKT pathways. J Hepatol 72: 761-773, 2020.
24. Komatsu K, Nakanishi Y, Nemoto N, Hori T, Sawada T and Kobayashi M: Expression and quantitative analysis of matrix metalloproteinase-2 and -9 in human gliomas. Brain Tumor Pathol 21: 105-112, 2004.
25. Xing P, Liao Z, Ren Z, Zhao J, Song F, Wang G, Chen K and Yang J: Roles of low-density lipoprotein receptor-related protein 1 in tumors. Chin J Cancer 35: 6, 2016.
26. Hu K, Yang J, Tanaka S, Gonias SL, Mars WM and Liu Y: Tissue-type plasminogen activator acts as a cytokine that triggers intracellular signal transduction and induces matrix metalloproteinase-9 gene expression. J Biol Chem 281: 2120-2127, 2006.
27. Shen H, Xu W, Luo W, Zhou L, Yong W, Chen F, Wu C, Chen Q and Han X: Upregulation of mdr1 gene is related to activation of the MAPK/ERK signal transduction pathway and YB-1 nuclear translocation in B-cell lymphoma. Exp Hematol 39: 558-569, 2011.
28. Meng X and Zhang S: MAPK cascades in plant disease resistance signaling. Annu Rev Phytopathol 51: 245-266, 2013.
29. Bian X, Liu R, Meng Y, Xing D, Xu D and Lu Z: Lipid metabolism and cancer. J Exp Med 218: e20201606, 2021.
30. Yancey PG, Blakemore J, Ding L, Fan D, Overton CD, Zhang Y, Linton MF and Fazio S: Macrophage LRP-1 controls plaque cellularity by regulating efferocytosis and Akt activation. Arterioscler Thromb Vasc Biol 30: 787-795, 2010.
31. Mutoh M, Komiya M, Teraoka N, Ueno T, Takahashi M, Kitahashi T, Sugimura T and Wakabayashi K: Overexpression of low-density lipoprotein receptor and lipid accumulation in intestinal polyps in Min mice. Int J Cancer 125: 2505-2510, 2009.
32. Gueddari N, Favre G, Hachem H, Marek E, Gaillard FL and Soula G: Evidence for up-regulated low density lipoprotein receptor in human lung adenocarcinoma cell line A549. Biochimie 75: 811-819, 1993,
33. Vasseur S and Guillaumond F: LDL Receptor: An open route to feed pancreatic tumor cells. Mol Cell Oncol 3: e1033586, 2016.
34. Miyabayashi K, Ijichi H, Mohri D, Tada M, Yamamoto K, Asaoka Y, Ikenoue T, Tateishi K, Nakai Y, Isayama H, *et al*: Erlotinib prolongs survival in pancreatic cancer by blocking gemcitabine-induced MAPK signals. Cancer Res 73: 2221-2234, 2013.
35. Rohlmann A, Gotthardt M, Hammer RE and Herz J: Inducible inactivation of hepatic LRP gene by cre-mediated recombination confirms role of LRP in clearance of chylomicron remnants. J Clin Invest 101: 689-695, 1998.
36. Ding Y, Xian X, Holland WL, Tsai S and Herz J: Low-density lipoprotein receptor-related protein-1 protects against hepatic insulin resistance and hepatic steatosis. EBioMedicine 7: 135-145, 2016.
37. Petersen C, Bell R, Klag KA, Lee SH, Soto R, Ghazaryan A, Buhrke K, Ekiz HA, Ost KS, Boudina S, *et al*: T cell-mediated regulation of the microbiota protects against obesity. Science 365: eaat9351, 2019.